Research article

Optimizing photocatalytic performance with Ag-doped ZnO nanoparticles: Synthesis and characterization

Atif Hussain [a,***], Shamaila Fiaz [a,b,*], Abdullah Almohammedi [c,**], Aqsa Waqar [a,b]

[a] Department of Physical Sciences, The University of Chenab, Gujrat, 50700, Pakistan
[b] Nanotechnology Lab, Department of Physics, University of Gujrat, Gujrat, 50700, Pakistan
[c] Department of Physics, Faculty of Science, Islamic University of Madinah, Madinah, 42351, Saudi Arabia

ABSTRACT

The development of nanotechnology has significantly impacted the improvement of photocatalytic performance of ZnO NPs. In this study synthesis of pure ZnO and Ag–ZnO nanoparticles via a co-precipitation method at varying Ag concentrations (1 %, 2 %, 3 %, 4 % and 6 %) to enhance their photo catalytic efficacy. X-ray diffraction (XRD) analysis estimates crystallite size which decreased by increasing Ag concentration, ranging from 30.6 nm (Pure ZnO) to 22.5 nm 6 % Ag-doped ZnO. Scanning electron microscopy (SEM) revealed decrease in particle size with increasing Ag content. UV–Vis spectroscopy indicating a narrowed band gap of optimal sample. Photocatalytic activity of the synthesized nanoparticles was evaluated using methylene orange (MO) dye degradation under light irradiation. The MO concentration exhibited a decrease with increasing irradiation time in the presence of photocatalysts. Recombination rate of NPs decreases by increasing the concentration of Ag i.e. 4%Ag dope ZnO NPs have lowest recombination rate and maximum degradation efficiency. FTIR analysis confirms the preparation of Ag-doped ZnO NPs. This improvement can be credited to the synergistic effect of Ag doping, leading to a narrowed band gap and potentially maximum degradation of MO by using Ag-doped ZnO NPs.

1. Introduction

Water is the basic need of life. Our body also consists of 60 % water and it is also used in different activities such as drinking, agriculture, industry, electricity production etc. Thus, we can say there is a large demand for water, especially clean water. About 71 % of Earth is composed of water. Fresh water is not only present on the surface of the earth but also present deep inside the earth in the form of aquifers. As already fresh water is limited and above this human begins are polluting these naturally occurring water resources due to their so-called development. Agricultural and industrial wastes are responsible for artificial pollution [1–5].

According to the U.N charter, it is the basic duty of the state to provide clean water to every citizen. But according to the report submitted to U.S organization about 748 million individuals do not have right to use clean water & because of this, wastewater treatment has become most important. For this purpose, different wastewater treatment technologies are used for example chlorination, distillation, extended aeration, oil water separation and so on. It is also observed that in water pollutants major contribution

goes to the organic impurities, especially organic dyes. It is estimated that about 7 lac ton dyes are produced by industries per year. Out of this figure only 12 % is wasted in suitable way, whereas 20 % is just flushed into the water [6–10]. Water pollutants usually includes organic wastes consisting of microbes [11], garbage and some nontoxic chemicals that can be treated easily [12]. Some other important defiles are in the form of acids like HCL,HF and so on that are extremely harmful [13]. Dyes are used in different industries such as paper printing, color fabricating, and photography and so on [10,14–17].

Phenols are another type of harmful aromatic organic pollutants which are produced from various types of industries such as petroleum, paper, preservative industries etc. These are most stable and reactive as well due to the presence of benzene rings in them, which are required to be degraded. Phenols are not as much harmful as pesticides or heavy metals are, and some time even they are used to kill microbes and against infectious micro organisms [18].

About 17–25 % harmful chemicals are left in water even after treatment. Thus, we require a latest and cost-effective technology. For this purpose, photocatalysis & green technology are topics of interests for researchers [19]. For this purpose different photocatalysts have been prepared and researchers are still working to prepare cost effective, industrial level, efficient photo catalyst [20,21]. Heterogeneous photocatalysis semiconductor oxides like TiO_2, WO_2, ZnO etc. are responsible for the degradation of organic con-taminants [22–26]. It should be noted that the band gap in the pure ZnO substance is considerably higher than 3.2 eV. Band gap energy of ZnO that is around 3.2 eV restricts its photo catalytic activity to the UV part of the light spectrum of wavelengths less than 387 nm. Therefore, ZnO has the capability to absorb less than five percent of the solar light and this has limited its applications in practice [27, 28].

The incorporation of metals such as Au, Ag, Co and Cu in ZnO has therefore become one of the well-established techniques for the achievement of the aforementioned objectives. Doping creates more energy levels intervals within ZnO band gap therefore leading to its reduction. This enables ZnO to absorb visible light with a longer wavelength, which adds to the light range of useful frequencies [29]. It may be pointed out that doping with selected metals such as silver (Ag) does bring out the phenomenon of surface Plasmon resonance (SPR). SPR causes formation of localized electric fields at the nanoparticle interface in the ZnO structure that increases light scattering and light absorption [30].

Among various dopants, silver nanoparticles (AgNPs) have garnered significant interest due to their unique properties. Incorpo-ration of AgNPs into ZnO should help improve the electronic conductivity of the photocatalyst and therefore enhance the ability of the photocatalyst to transport charges throughout the doped ZnO material. Another advantage that favors the application of AgNPs is the chemical stability that they demonstrate, thus guaranteeing the effectiveness of the photocatalyst in the long run. Silver itself has inherent catalytic and antimicrobial properties which are likely to provide extra functions to doped ZnO photo catalyst [31].

There are different approaches towards synthesizing functional ZnO nanoparticles with or without functionalization. Common techniques include Spray pyrolysis, electrochemical methods, Thermal decomposition, Vapor transport processes, Sonochemical routes. Among them, the co-precipitation method is one of the most popular in synthesizing Ag-doped ZnO photocatalysts due to its advantages such as simplicity and cost-effectiveness [32].

In a study by Ref. [33], the photo catalytic degradation of the reactive blue 21 dye was studied using the Ag-doped ZnO nano-particles synthesized with co precipitation method. It has been established that their findings recorded high photo degradation effi-ciency under UV light and other properties such as efficient dye decolorization at lower pH level [34]. Analyzed the photo degradation of Safranin O, Rhodamein B and methyl Oranda by using Ag–ZnO NPs fabricated through co precipitation technique of different Ag dopant concentrations (0. 2-2%). According to their findings they affirmed that the ZnO material with doping had enhanced photo-catalytic activity.

The novelty in our work is reflected by the Chemical Coprecipitation method that is simple, easy to perform, time saving, less hazardous and does not use high temperatures as hydrothermal method does. The synthesized material shown nanorods like morphology for optimal sample and spherical morphology for non-optimal samples that participated in successful enhanced degra-dation of MO dye. In comparison to previous articles, no reports properly depicted that type of rod-like morphology that our optimal sample showed and hence it will have better and greater surface area and active sites for degradation of harmful pollutants.

2. Materials and methods

Using the co-precipitation method, the synthesis of both pure and Ag-doped ZnO nanoparticles was successfully carried out. Analytical grade reagents were used without further purification. Zinc nitrate hexa-hydrate ($Zn(NO_3)_2.6H_2O$) was used as the source of zinc oxide (ZnO) and silver nitrate ($AgNO_3$) was employed for the purpose of incorporating silver (Ag) dopant into the ZnO nano-particles, Methyl orange dye was used as organic pollutant in solution of distilled water. All these materials were available at the University of Chenab with absolute purity (>99 %, Sigma Aldrich). Ethanol and deionized water were used for washing the product to eliminate any additional by-products that could form during the synthesis course.

2.1. Synthesis of ZnO nanoparticles via Co-precipitation

ZnO nanoparticles were prepared by using Co-precipitation method. A 0.375 M aqueous solution of zinc nitrate ($Zn(NO_3)_2$) which was prepared by dissolving 3 g of the precursor in 80 mL of deionized water under constant magnetic stirring for a period of 60 min at a temperature of 80 °C. A separate solution of sodium hydroxide (NaOH) was made by dissolving 6 g in 20 mL of deionized water thereby stirring it for 30 min. The NaOH solution added dropwise to the stirred zinc nitrate solution followed by heating at 80 °C for 60 min. NaOH plays a critical role in controlling the reaction environment and the final properties of the nanoparticles. After 60 min stirring, the precipitates was allowed to settle for 16 h at room temperature. The white precipitate washed with deionized water with 3–4 times
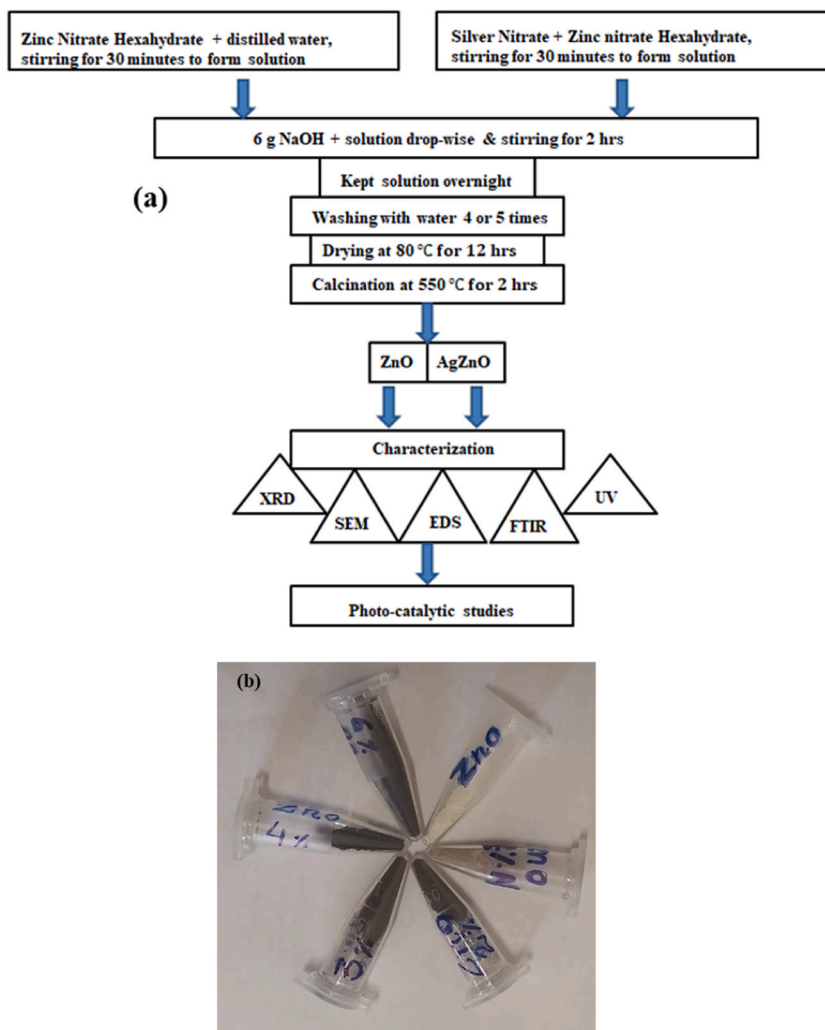
Fig. 1. (a) Flow chart of the experimental procedure, **(b)** Synthesized ZnO and Ag doped ZnO.

Table 1
Conditions for synthesis of ZnO and Ag doped ZnO nanoparticles.

Sr#.	Sample	Precursors	Method	Reaction Temperature	pH of reaction	Calcination temperature
1.	**ZnO**	Zinc Nitrate, NaOH	Coprecipitation	80° C	10	550° C, 2h
2.	**1%Ag–ZnO**	Zinc Nitrate, NaOH, silver nitrate	Coprecipitation	80° C	10	550° C, 2h
3.	**2%Ag–ZnO**	Zinc Nitrate, NaOH, silver nitrate	Coprecipitation	80° C	10	550° C, 2h
4.	**3%Ag–ZnO**	Zinc Nitrate, NaOH, silver nitrate	Coprecipitation	80° C	10	550° C, 2h
5.	**4%Ag–ZnO**	Zinc Nitrate, NaOH, silver nitrate	Coprecipitation	80° C	10	550° C, 2h
6.	**6%Ag–ZnO**	Zinc Nitrate, NaOH	Coprecipitation	80° C	10	550° C, 2h

to eliminate any other impurities. The final washing was done using ethanol to optimize the removal of water soluble impurities. ZnO precipitate was filtered off and put in a drying oven at 80° for 24 h. Lastly, the dried ZnO powder was calcined at 550 °C in muffle furnace for about 2 h. After grinding and crushing, the final product of ZnO NPs were obtained as presented in Fig. 1(a).

2.1.1. Synthesis of Ag-doped ZnO nanoparticles

ZnO nanoparticles with different concentrations of silver (1 %, 2 %, 3 %, 4 % and 6 %) were synthesized via Co precipitation method. For 1 % Ag doping, 2.97 g of zinc nitrate hexa-hydrate, mixed it in 70 ml of distilled water and 0.03 g of silver nitrate was dissolved in 10 ml of distilled water. Then both the solutions were stirred for half an hour to dissolve all the components. Then after half an hour stirring silver nitrate solution was mixed with zinc nitrate solution. The both the solutions were stirred for half an hour at 80°C. After 60 min stirring, silver nitrate solution was mixed with zinc nitrate solution. A sodium hydroxide solution was made up by
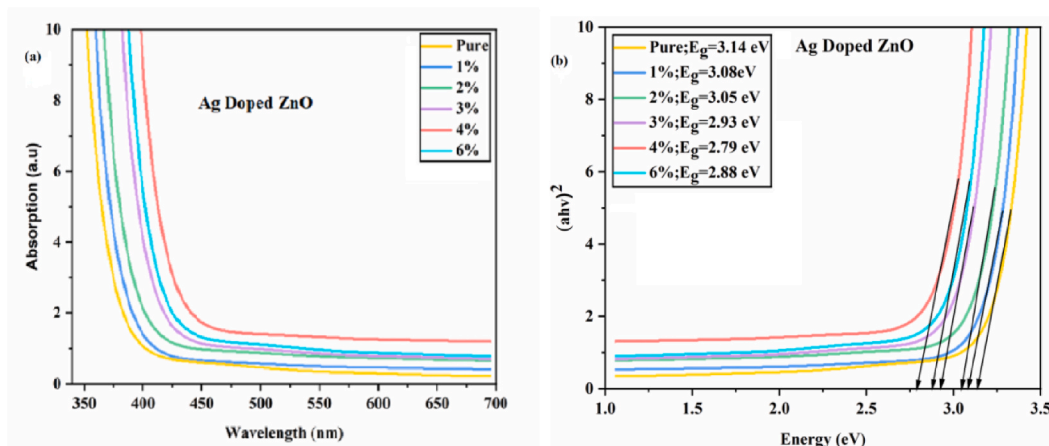
Fig. 2. (a) Comparison of UV–visible Spectra of pure ZnO and Ag–ZnO nanoparticles (**b**) Comparison of Band gap Energies of pure ZnO and Ag -ZnO nanoparticles.

dissolving 6 g of NaOH in 20 ml of deionized water and allowed to stir for 30 min. An aqueous solution of NaOH was then added dropwise to above-described mixture of zinc nitrate and silver nitrate under constant stirring at 80 °C for 1h. This step ensures aggregation of the Ag-doped ZnO nanoparticles with enhanced co-precipitation. After stirring, reaction mixture was allowed to stele down for 16 h at room temperature. The black precipitates were washed with deionized water for 3–4 times. Ag-doped ZnO precipitate was then dried over at temperature of about 80 °C for 24 h. Lastly the dried powder was finally calcined in Muffle furnace at a temperature of 550 °C for 2 h. Thus, in addition to increasing the degree of crystallinity, this treatment helps to remove the last remnants of organic contaminants. The color of the material also changes from gray for 1 % Ag-doped ZnO sample to jet black for samples for higher dopant concentrations as shown in Fig. 1(b). Table 1 shows the Conditions for synthesis of ZnO and Ag doped ZnO nanoparticles.

2.2. Characterization techniques

Synthesized nanoparticles (pure ZnO, and Ag doped ZnO) were subjected to various characterization techniques to understand their properties. Description of the optical properties of the nanoparticles was done by using the UV–visible dual beam spectrophotometer. The band gap energy is essential for photo catalytic activity. Xenon lamp was used as the source of excitation for the for characterization of photoluminescence properties of the synthesized nanoparticles. In the photo catalytic process, the solution was exposed to light from a 100W incandescent lamp during the experiment. The functional groups absorbed on the exterior of prepared nanoparticles were analyzed by Fourier Transform Infrared Spectroscopy commonly known as FTIR. Crystal structure characterizations were done by using an X-ray diffractometer, and the pattern was obtained using Cu-Kα radiation source ($\lambda = 0.15405$ nm) at 40 kV. Characterization of synthesized silver nanoparticles was done by scanning electron microscopy (SEM) for the purpose of identifying the shape (morphology) and size of the nanoparticles. Energy dispersive X-ray Fluorescence spectroscopy (EDX) analysis was conducted to identify elemental content in the prepared nanoparticles.

2.3. Evaluation of photo catalytic activity against methyl orange dye

Specifically, degradation of Methyl orange (MO) dye, which is among the most well-known pollutants, was used to determine the photocatalytic efficiency of the prepared ZnO and Ag–ZnO nanoparticles. MO is an anionic azo dye and is poisonous to plants because of its carcinogenic properties. It is also harmful for humans, it can provoke irritation of eyes, skin, and gastrointestinal tract if inhaled or swallowed [6]. It's pH range is 2.8–3.8. The photo catalytic degradation performance of the synthesized nanoparticles for MO dye was tested by examining the irradiation effect under visible light. Methyl orange dye was dissolved in distilled water to give a solution of 500 mL with a concentration of 10 mg/L. This concentration is typical of the levels of organic pollutants that one is likely to expect in wastewater. Later, the solution was sonicated for 30 min with the aim of achieving homogeneity of the dye molecules within the solution. In each experiment, where a particular synthesized nanoparticle sample was involved, 100 mL of the prepared MO dye solution was employed. Reaction mixture wherein the photo-catalyst was immersed was exposed to visible light irradiation for a cumulative time of 120 min using the photo-catalytic reactor. To determine the photocatalytic efficiency of the synthesized nanoparticles, photo-degradation experiments were conducted and the change in the concentration of MO dye during irradiation was analyzed. Normally one must use UV–vis spectroscopy for this as the absorption band of the dye solution is known to decrease with degradation. The percentages of MO dye degradation at corresponding concentrations of the nanoparticles will help determine the catalytic efficiency of the nanoparticles using this equation.
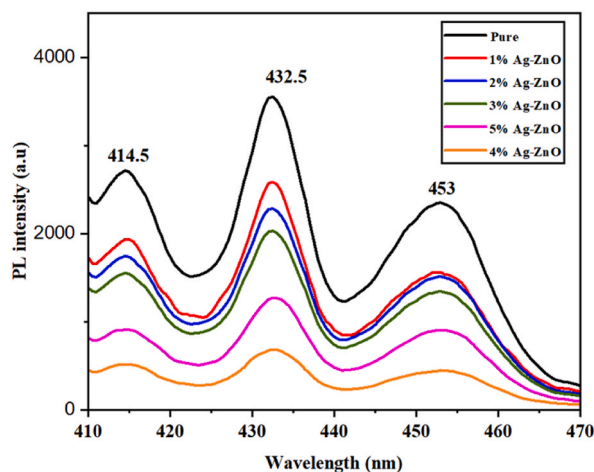
Fig. 3. Pl spectra of pure and Ag doped ZnO.

$$\text{Photo catalytic Efficiency} = \frac{C_{o-}C_t}{C_o} \times 100$$

3. Results and discussion

3.1. UV–visible spectroscopy

UV–Visible spectroscopy is used for understanding of the electronic composition and optical features of the semiconductors. We have prepared pristine ZnO and Ag– ZnO nano particles, so we will discuss properties of pure ZnO and Ag– ZnO NPs.

The absorption in UV–visible spectra of ZnO, 1 %,2 %,3 %,4 % and 6 % Ag–ZnO Nano particles are shown in Fig. 2a. The spectrum is observed between absorbance intensity (a.u) and wavelength (nm).

From Fig. 2 (a) it can be observed clearly that there is variation in wavelength of doped samples. Pure samples lie within the UV range of electromagnetic spectra. Whereas with increasing doping percentage wavelength will also increases, so wavelength is shifted from UV to visible region [35,36].

$$\alpha h\upsilon = A\left(h\upsilon \ - \ E_g\right)^n \tag{2}$$

The band gap can be measured by using equation (2). The observed band gaps are 3.14 eV, 3.08 eV, 3.05 eV, 2.93 eV, 2.79 eV and 2.88 eV for Pure ZnO, 1 %, 2 %, 3 %, 4 % and 6%- Ag doped ZnO, respectively. Reduction in band gap occurs due to increase in dopant concentrations.

It can be seen from UV graphs that there are no separate peaks for AgNO$_3$, this is because AgNO$_3$ is an ionic compound and not a colored material on its own, its solution is pale yellow in color. UV–Visible Spectroscopy deals with the absorption of UV and visible light by molecules; this leads to a promotion of electrons from the lower energy level to the higher energy level. Since silver nitrate is an ionic compound, it has no conjugated pi bonds and therefore it cannot absorb UV or visible light. There are a few other reasons why silver might not show a clear peak in our Ag-doped ZnO's UV–Vis spectrum. In case of low silver content its signal can be completely overridden by ZnO absorption signal. Also, the incorporation of silver dopants into the position of ZnO may not lead to the formation of another peak. The size of the particles is also important, bigger agglomerates of the silver particles are detected better than abstract, very fine, but highly charged silver ions [37]. Optical properties of Nanoparticles are directly related to the size of the Nanoparticles. As the size of the particle reduces the quantum confinement increases. So, with decrease in size, quantum confinement will be greater due to which energy band gap will also increase. As the wavelength goes on increasing, particle size will also increases which causes reduction in band gap [38]. Above mentioned graphs prove this statement, so in case of this series Ag–ZnO-4 have maximum wavelength hence minimum energy band gap. According to UV results this is the optimal sample.

3.2. Photoluminescence (PL) emission spectrum

To determine the inside defects produced in the synthesized prepared ZnO Nano materials with & without using Ag, photo-luminescence spectroscopy was used. The excitation wavelength and morphology of the prepared ZnO materials play the main role in the production of energy position, intensity and the shape of the peaks. The PL spectra of all samples at room temperature with 350 nm excitation wavelength have been portrayed in Fig. 3.

3.2.1. PL emission spectrum of Ag doped ZnO

The spectrum in Fig. 3 shows a broad peak centered about 430 nm (see). This peak is likely due to the emission of light from the
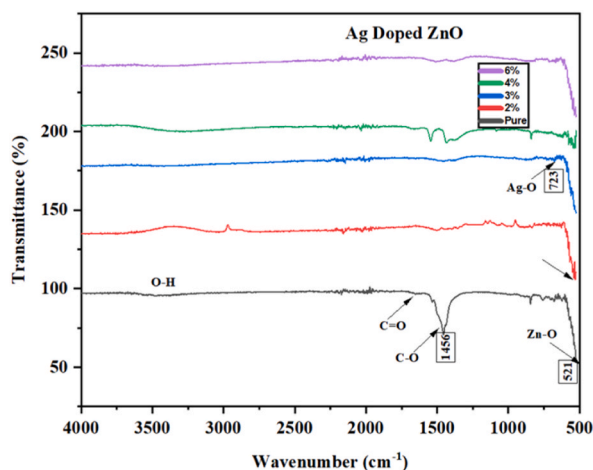
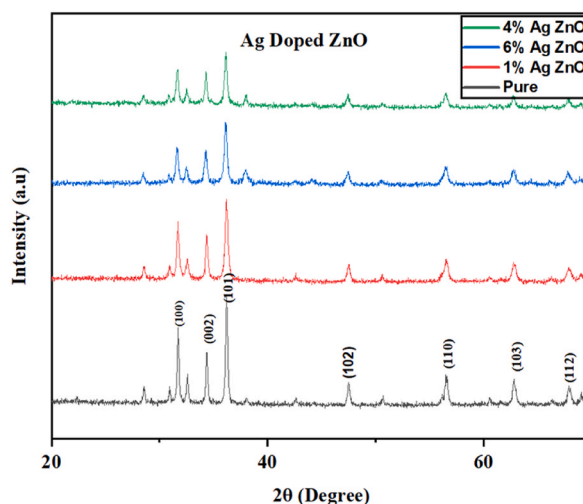**Fig. 4.** FTIR spectrum of Pure and Ag–ZnO NPs.

**Fig. 5.** XRD Pattern of Pure and Ag doped ZnO nanoparticles.

band gap of the material. Band gap is the energy difference between the valence band and the conduction band.

Intensity of the peak decreases with increasing concentration of silver (Ag). The intensity of PL decrease by increasing concentration of Ag. These states might act as intermediate traps for the excited electrons, facilitating non-radiative recombination (heat generation) instead of radiative recombination (light emission). As the Ag concentration increases, the surface area of the material might also increase. Surface defects can act as recombination centers, reducing the overall PL intensity. Silver ions (Ag+) within ZnO structure could interact with the excited states of the host material, reducing the probability of radiative recombination and hence the PL intensity [37,39,40].

3.3. FTIR spectrum of Ag doped ZnO nanoparticles

FTIR spectroscopy is a technique used to identify functional groups in a molecule by analyzing its infrared absorption pattern. Different chemical bonds vibrate at specific frequencies when irradiated with infrared light. By measuring the absorbed frequencies, we can identify the chemical functional groups in the sample.

In Fig. 4, several peaks are labeled with the functional group they represent. Such as 3400-3200 cm^{-1}, O–H stretching vibration,1600-1400 cm^{-1} C=O,400-650 cm^{-1} M – O stretching vibration which is due to metal oxides. Peak at 420 cm^{-1} can be due to Zn–O stretching, indicating the presence of zinc oxide [41]. ZnO nanoparticles can also chemisorb water molecules from the surrounding since they have a high surface area. These water molecules may be involved in OH stretching and bending in the FTIR spectrum of the samples. Broad peaks in the transmittance region of 3200–3600 cm^{-1} is due to the O–H stretching.
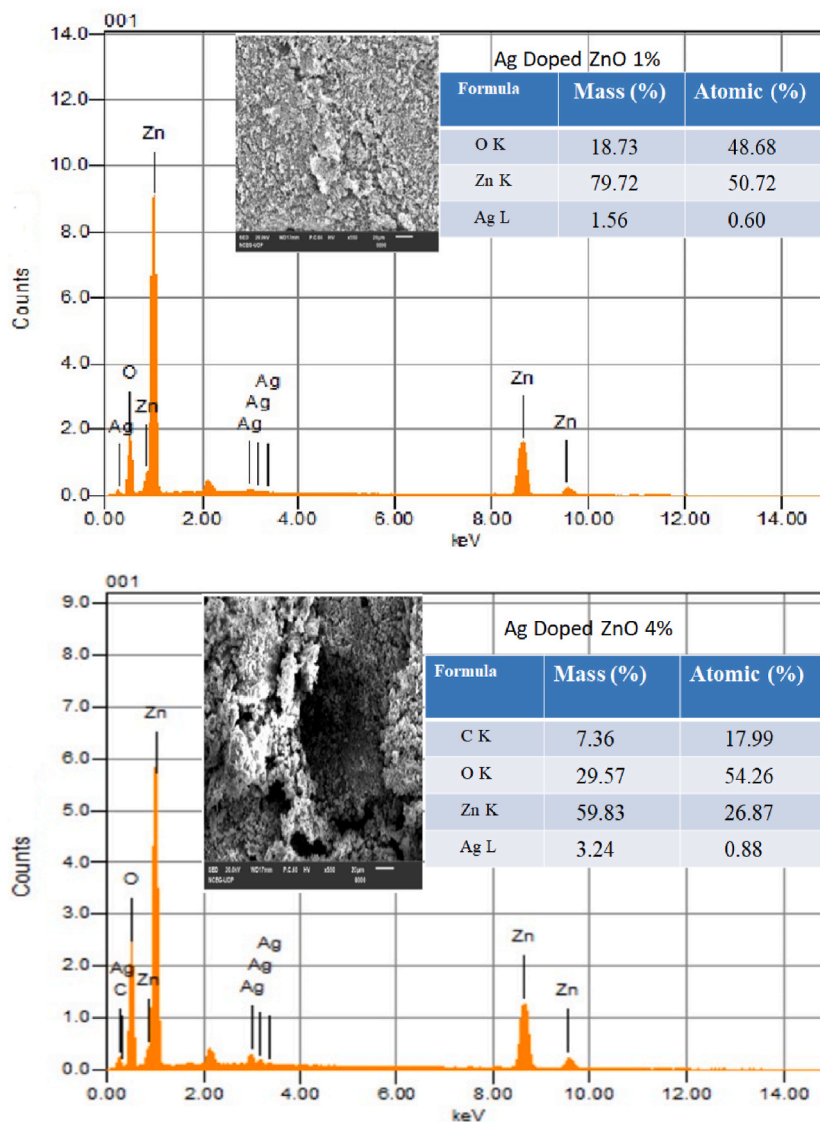
Fig. 6. 1: Energy-Dispersive X-ray Spectroscopy (EDS) analysis of (Ag–ZnO-1). 2: Energy-Dispersive X-ray Spectroscopy (EDS) analysis of (Ag–ZnO-4). 3: Energy-Dispersive X-ray Spectroscopy (EDS) analysis of (Ag–ZnO-6).

3.4. XRD analysis of Ag doped ZnO nanostructures

Fig. 5 shows the X-ray diffraction (XRD) patterns corresponding to pristine ZnO and ZnO doped with varying silver (Ag) concentrations. These patterns offer a crystallographic fingerprint of the materials.

The observed peaks at specific 2θ angles correspond to the constructive interference of X-rays diffracted by specific crystallographic planes within the material. The relative intensities of these peaks are crucial for determining the unit cell parameters and the crystal structure of the material [42]. A progressive decrease in intensity of the ZnO peaks is observed with increasing Ag dopant concentration. This signifies a corresponding rise in the silver content within the ZnO crystal lattice that disturbed the crystal lattice. Strong and wide pattern of diffraction peaks of pristine ZnO suggest typical peaks of hexagonal wurtzite structure (JCPDS card no: 00-005-0664) at 31.7°, 34.4°, 36.2°, 47.5°, 56.6°, 62.8°, 67.9° matching with the reflection planes (100), (002), (101), (102), (110), (103), (112), respectively [43]. The crystal sizes are 30.6 nm for Ag–ZnO-0%, 27.02 nm for Ag–ZnO-1%, 26.1 nm for Ag–ZnO-4% and 22.5 nm for Ag–ZnO-6%.

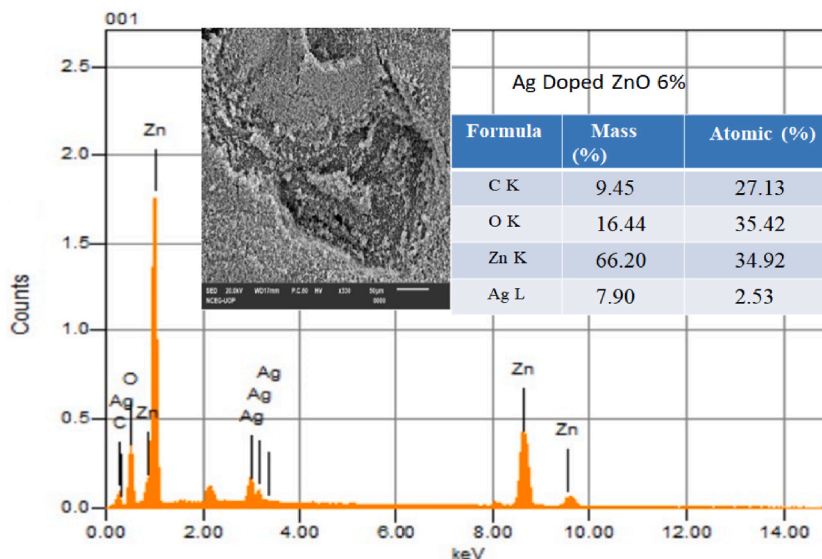| Ag Doped ZnO 6%		
Formula	**Mass (%)**	**Atomic (%)**
C K	9.45	27.13
O K	16.44	35.42
Zn K	66.20	34.92
Ag L	7.90	2.53

Fig. 6. (*continued*).

3.5. EDS analysis

EDS is a technique used to identify elemental composition of a sample by measuring the characteristic X-rays emitted by its atoms. The presence of carbon in EDS spectra was confirmed by characterization laboratory that they used carbon tape on which sample was pasted for the analysis.

Fig. 6 shows that sample is primarily consist of zinc (Zn) (59.83 % mass), oxygen (O) (29.57 % mass), and silver (Ag) (3.24 % mass). The peaks in the graph correspond to the characteristic X-rays emitted by the elements in the sample. For example, the peak at around 3.0 keV corresponds to the L-alpha X-ray of silver (Ag L). For Ag–ZnO 1 % as shown in Fig. 6(1):the sample is primarily composed of zinc (Zn) (79.72 % mass), oxygen (O) (18.73 % mass), and silver (Ag) (1.56 % mass). For Ag–ZnO 4 % as displayed in Fig. 6(2): sample is primarily composed of zinc (Zn) (59.83 % mass), oxygen (O) (29.57 % mass), and silver (Ag) (3.24 % mass). For Ag–ZnO 6 %: Fig. 6 (3) shows that the sample is primarily composed of zinc (Zn) (66.20 % mass), oxygen (O) (16.44 % mass), and silver (Ag) (7.90 % mass).

3.6. SEM analysis of Ag doped ZnO

Scanning electron microscopy (SEM) analysis was employed to investigate the influence of noble metal doping on the morphology of pristine ZnO nanoparticles (ZnO NPs) and Ag-doped ZnO nanoparticles. Fig. 7 reveals surface morphology of all samples. ZnO showed cylindrical and irregular spherical shapes whereas the doping of silver in ZnO successfully enhanced the morphology. For 4 % Ag doped ZnO, cylindrical and hexagonal rod-like structures are formed whereas for 1 % Ag doped ZnO and 6 % Ag doped ZnO, spheres are formed [44]. As it is exhibited from images, Ag–ZnO-4 has the best morphology, so this one is the best sample in this series. Ag-doped ZnO samples, demonstrating good agreement with the observations from X-ray diffraction (XRD) analysis. Using Image J software, the average particle size is calculated as for pure ZnO is 85 nm, Ag–ZnO 1 % is 78.5 nm, Ag–ZnO 4 % is 50.5 nm and Ag–ZnO 6 % 65 nm. The average particle size of pure ZnO and 6 % Ag doped ZnO is shown in Fig. 7e and f.

3.7. Photocatalytic activity

Photocatalytic activity of the prepared sample by performing a simple experiment. For this experiment, a Methyl Orange (MO) dye was used and execute the degradation testing to check the efficiency and stability of Ag doped ZnO NPs.

3.7.1. Methyl orange dye

Methyl orange acts as a pH indicator, changing color across a specific pH range. It transitions from red in acidic solutions (below pH 3.1) to orange in weakly acidic solutions (around pH 4.3), and finally to yellow in basic solutions (above pH 4.4). Therefore, it doesn't have a single defined pH value. Methyl orange has a molecular weight of approximately 327.33 g/mol.

The purpose of the current study is to evaluate photocatalytic efficiency of a prepared nanoparticles to decolourize the methylene orange (MO) dye. For photodegradation, we have prepared a solution by adding 5 mg of methyl orange dye powder in 500 ml of distilled water and did stirring for 30 min in dark, so that dye mix well into the water. Then we took the first reading in unlit environment. Photocatalytic degradation reaction specifications are as follows: Temperature: 30 °C (normal), light source power: 450 W mercury high pressure lamp, and distance between the light source and reaction mixture: 15 cm. S For each sample, we took 100 ml
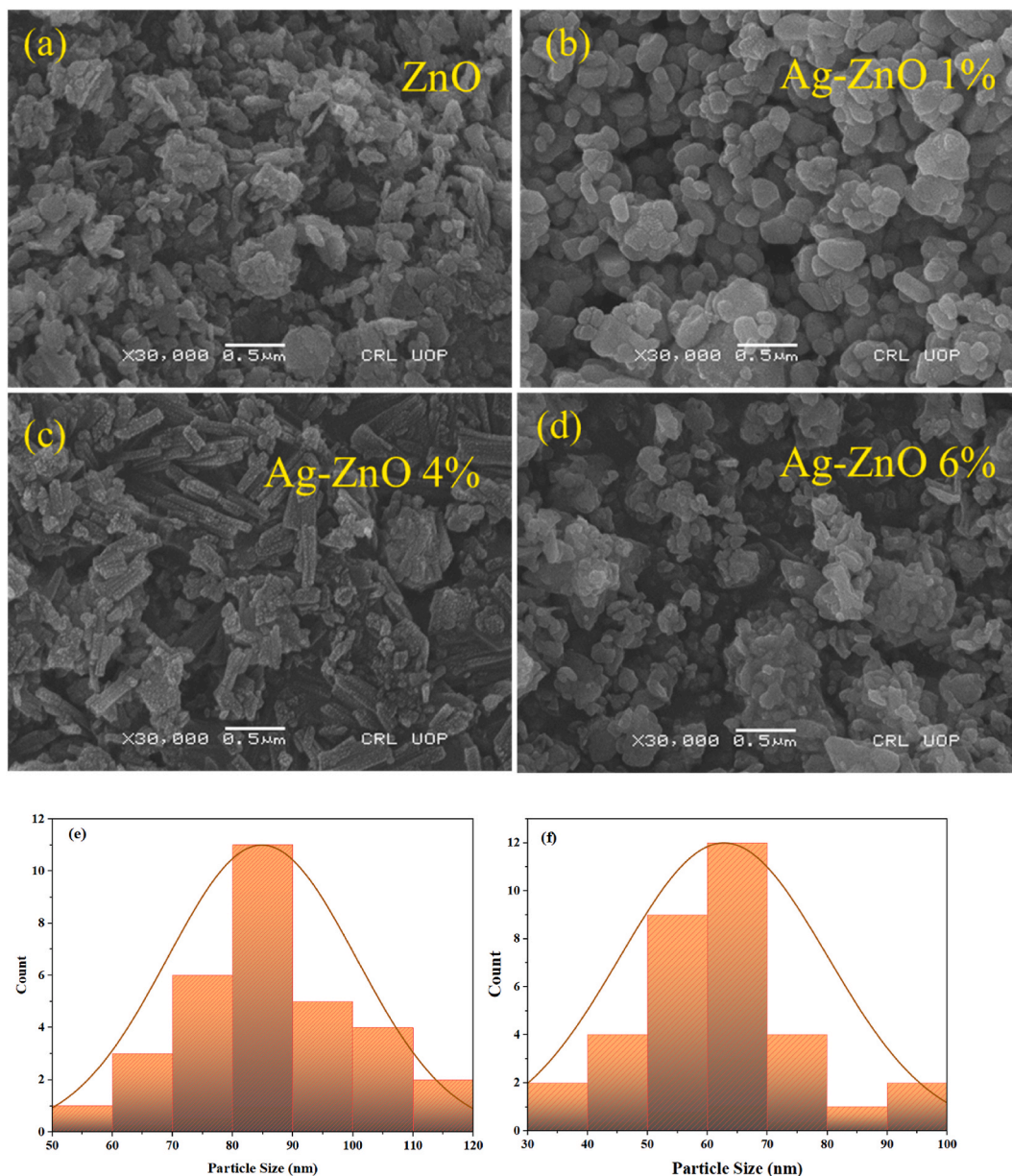
Fig. 7. SEM images of (a) ZnO, (b) Ag–ZnO-1, (c) Ag–ZnO-4 (d) Ag–ZnO-6 (e) Histogram of ZnO, (f) Histogram of Ag–ZnO-6.

taken from the preliminary impurity solution. Then we introduced an accurately calculated amount, 15 mg of nanomparticles into the impurity solution, ensuring careful exposure to an unlit environment [45]. The agitating process is continued for a period of 30 min at room temperature. With the help of high-pressure mercury lamp of 450 W photocatalysts were subjected to irradiation. Consequently, solution experiences irradiation by using a UV–visible light source for a period of 120 min. Ultraviolet–visible spectrometer analysis is directed at regular gaps of 30 min. By using a UV–visible spectroscopy wavelength spectra from 200 to 900 nm were obtained. A visible change in solution's color is observed, it is shifted from dark orange to a approximately colorless solution with the passage of time.

$$\text{Degradation}\% = \frac{C_o - C_t}{C_o} \times 100$$

C_o is used for initial concentration of methyl orange dye and C_t used for concentration of MO dye after specific time of photo-degradation (see). Fig. 8a shows the comparison plot about the degradation of MO dye between pure ZnO and Ag doped ZnO samples. In this figure, the purple line, as indicated as "pure" in the legend elaborates the degradation performed by pure ZnO sample (32.5 %) against MO dye in 120 min 1 %, 2 %, 3 %, 6 % and 4 % Ag doped ZnO nanoparticles showed 49.3 %, 57.4 %, 66.8 %, 77.7 % and 86.5 % degradation respectively of MO dye in a time span of 120 min. Comparison of photocatalytic degradation percentage of Ag
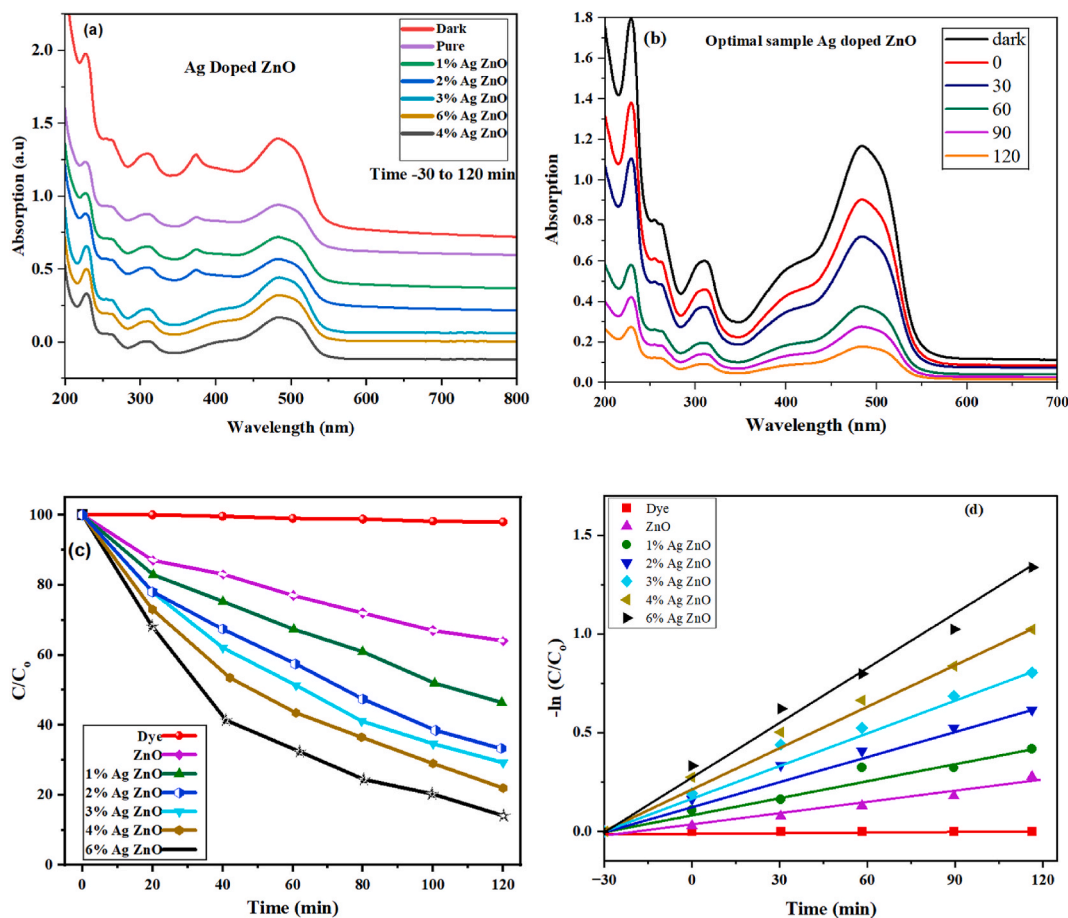
Fig. 8. (a) UV–visible absorbance spectra of MO in the presence of all samples of Ag–ZnO **(b)** UV–visible absorbance spectra of MO in the presence of optimal sample of Ag–ZnO-4 **(c)** Plot of degradation v/s time (min) **(d)** Kinetics relationship of ln(C/C0) v/s irradiation time for Ag–ZnO NPs.

Table 2
Morphological and optical comparisons with the degradation efficiency of photocatalysts.

Sr. No.	Sample	Average Particle Size by XRD/SEM (nm)	Pollutant	Degradation %	Morphology	Band gap
1.	Pure ZnO	30.6/83.5	MO Dye	49.3 %	Spherical	3.14 eV
2.	Ag–ZnO 1 %	27.02/78.5	MO Dye	66.8 %	Spherical	3.08 eV
4.	Ag–ZnO 4 %	26.01/50.5	MO Dye	86.5 %	Nanorods	2.79 eV
5.	Ag–ZnO 6 %	22.5/68.5	MO Dye	77.7 %	Spherical	2.88 eV

Table 3
Comparison of the degradation percentage of Ag doped ZnO with previous studies.

Sr no.	Photocatalyst	Pollutant	Degradation %	References
1	ZnO	MB dye	96.2 %	[48]
2	Mn doped WO_3	MB dye	79 %	[49]
3	Cu-doped ZnO	MG dye	75 %	[50]
4	Mn-doped ZnO	MG dye	66.4 %	[51]
5	Ag–ZnO	MO dye	86.5 %	Current work

doped ZnO with previous study as shown in Table 3 (see).

All above graphs proves that Ag–ZnO-4 is the optimal sample as it degraded the dye almost 86.5 % as compared to other samples, so this one is the best sample of this series [46]. Table 2 shows the Morphological and optical comparisons with the degradation efficiency of photocatalysts.
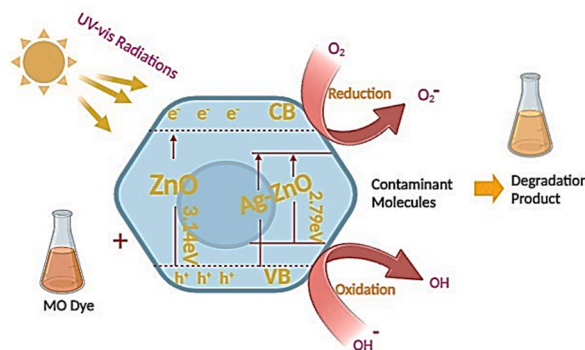
Fig. 9. Proposed possible Photocatalytic Mechanism for degradation of MO dye.
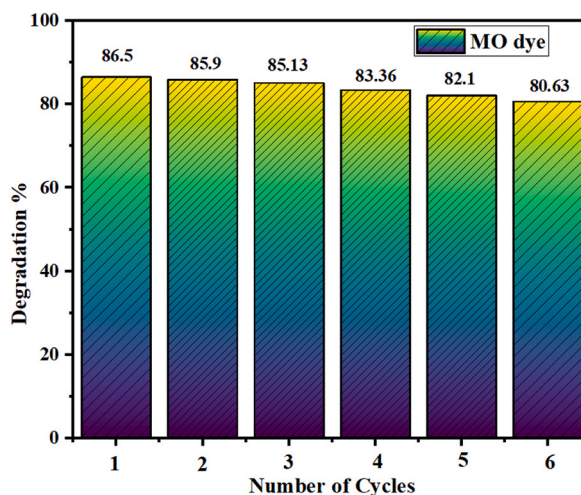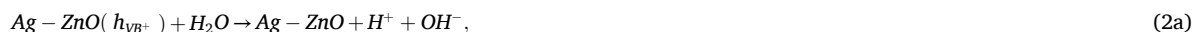

Fig. 10. Cyclic test against MO dye by optimal 4 % Ag doped ZnO nanoparticles for 6 cycles.

3.7.2. Possible photocatalytic degradation mechanism

With a bandgap of 3.14 eV, pure ZnO is a promising semiconductor for use as an effective visible light-driven photocatalyst. We successfully lowered the bandgap of pure ZnO from 3.14 to 2.79 eV by adding Ag at varying concentrations. This was made possible by introduction of new energy levels beneath and above the valence band and conduction band, respectively. Doping reduces recombination time of charge carriers by creating energy traps between conduction band and valence band, whereas the specific site eases the surface redox reaction [47]. The proposed Photocatalytic Mechanism for degradation of MO dye is presented in Fig. 9.

$$Ag - ZnO + h\nu \rightarrow Ag - ZnO(e_{CB^-} + h_{VB^+}), \tag{1}$$

$$Ag - ZnO(h_{VB^+}) + H_2O \rightarrow Ag - ZnO + H^+ + OH^-, \tag{2a}$$

$$Ag - ZnO(e_{CB^-}) + O_2 \rightarrow Ag - ZnO + O_2^{\bullet}, \tag{3}$$

$$Ag - ZnO(h_{VB^+}) + OH^- \rightarrow Ag - ZnO + OH^{\cdot}, \tag{4}$$

$$MO\ Dye + O_2^{\bullet} \rightarrow degradation\ products + CO_2 + H_2O, \tag{5}$$

$$MO\ Dye + OH^{\bullet} \rightarrow degradation\ products + CO_2 + H_2O. \tag{6}$$

3.7.3. Recycling stability test for 4 % Ag doped ZnO

The optimal sample, 4 % Ag doped ZnO showed 86.5 % degradation against MO dye in a total time span of 120 min. After 120 min, the catalyst was recovered by washing of solution with DI water and by centrifugation, then dried in hotair oven. The catalyst's efficiency was evaluated for consecutive 6 cycles to verify its promising behavior, material's integrity and stability against MO dye. 4 % Ag doped ZnO showed 86.5 %, 85.9 %, 85.13 %, 82.1 % and 80.63 % degradation for consecutive 6 cycles as shown in Fig. 10. Interestingly, there was only 5.87 % degradation loss in 6 cycles that proved its promising behavior.

4. Conclusion

Monodispersed Nano crystals of ZnO with and without silver doping were fabricated via a chemical coprecipitation route. X-ray diffraction (XRD) and UV–visible (UV–Vis) spectroscopy were done to characterize the crystalline structure, optical properties, and band gap of the synthesized materials. XRD and scanning electron microscopy (SEM) analyses confirmed hexagonal wurtzite crystal phase of the obtained nanoparticles. XRD data revealed average crystallite size ranging from 20 nm to 35 nm. Furthermore, these studies demonstrated successful incorporation of silver (Ag) dopant ions into the ZnO lattice with uniform distribution throughout the samples. The observed band gaps are 3.14 eV, 3.08 eV, 3.05 eV, 2.93 eV, 2.79 eV and 2.88 eV for Pure ZnO, 1 %, 2 %, 3 %, 4 % and 6%-Ag doped ZnO, respectively. This research reveals a higher silver doping percentage resulted in a decrease in particle size. Photocatalytic activity of ZnO nanoparticles was significantly improved with Ag doping. Among the synthesized samples, Ag– ZnO-4 displayed the highest photodegradation efficiency for methylene orange (MO) under UV irradiation. The degradation performed by pure ZnO sample (32.5 %) against MO dye in 120 min 1 %, 2 %, 3 %, 6 % and 4 % Ag doped ZnO nanoparticles showed 49.3 %, 57.4 %, 66.8 %, 77.7 % and 86.5 % degradation respectively of MO dye in a time span of 120 min and just 5.87 % loss in degradation was observed after consecutive 6 cycles. So, the 4 % Ag doped ZnO showed best optical, morphological and catalytic properties.

CRediT authorship contribution statement

Atif Hussain: Writing – review & editing. **Shamaila Fiaz:** Writing – review & editing. **Abdullah Almohammedi:** Formal analysis. **Aqsa Waqar:** Writing – review & editing.

Declaration of competing interest

The authors declare that they have no known competing financial interests or personal relationships that could have appeared to influence the work reported in this paper.

Acknowledgments

References

[1] D. Mishra, M. Srivastava, Low-dimensional nanomaterials for the photocatalytic degradation of organic pollutants, in: Nano-Materials as Photocatalysts for Degradation of Environmental Pollutants, Elsevier, 2020, pp. 15–38.
[2] A. Boutalbi, et al., Photocatalytic dye degradation efficiency and reusability of potassium polyacrylate hydrogel loaded Ag@ ZnO nanocomposite, Transit. Met. Chem. 48 (5) (2023) 353–363.
[3] S. Meneceur, et al., High-efficiency photocatalytic degradation of antibiotics and molecular docking study to treat the omicron variant of COVID-19 infection using biosynthesized ZnO@ Fe3O4 nanocomposites, Phys. Scripta 98 (11) (2023) 115926.
[4] D. Barani, et al., Biomass-mediated synthesis of ZnO and Mg@ ZnO nanoparticles for enhancing the degradation of m-toluidine and p-toluidine, Biomass Conversion and Biorefinery 13 (8) (2023) 7311–7318.
[5] A. Tabet, et al., One Post biosynthesis of novel ternary nanocomposite ZnO/CuO/Cu2MgO3 for enhancing photocatalytic degradation of bromocresol green in wastewater, J. Cluster Sci. 35 (3) (2024) 765–777.
[6] N. Wang, et al., Microfluidic reactors for photocatalytic water purification, Lab Chip 14 (6) (2014) 1074–1082.
[7] L. Hamza, et al., Biosynthesis of ZnO/Ag nanocomposites heterostructure for efficient photocatalytic degradation of antibiotics and synthetic dyes, Z. Phys. Chem. (0) (2024).
[8] A.H. Gharbi, et al., Green synthesis of ZnO@ SiO2 nanoparticles using Calligonum comosum L. extract: an efficient approach for organic pollutant degradation in wastewater, Biomass Conversion and Biorefinery (2023) 1–12.
[9] B. Gherbi, et al., Effect of pH value on the bandgap energy and particles size for biosynthesis of ZnO nanoparticles: efficiency for photocatalytic adsorption of methyl orange, Sustainability 14 (18) (2022) 11300.
[10] I. Ben Amor, et al., Sol-gel synthesis of ZnO nanoparticles using different chitosan sources: effects on antibacterial activity and photocatalytic degradation of AZO Dye, Catalysts 12 (12) (2022) 1611.
[11] M.B. Tahir, M. Sagir, K. Shahzad, Removal of acetylsalicylate and methyl-theobromine from aqueous environment using nano-photocatalyst WO3-TiO2@ g-C3N4 composite, J. Hazard Mater. 363 (2019) 205–213.
[12] P. Goel, Water Pollution: Causes, Effects and Control, 2006. New age international.
[13] E.M. Carstea, et al., Fluorescence spectroscopy for wastewater monitoring: a review, Water Res. 95 (2016) 205–219.
[14] X. Fei, D. Zekkos, L. Raskin, Archaeal community structure in leachate and solid waste is correlated to methane generation and volume reduction during biodegradation of municipal solid waste, Waste Management 36 (2015) 184–190.
[15] A. Boutalbi, et al., Synthesis of Ag nanoparticles loaded with potassium polyacrylate hydrogel for rose bengal dye removal and antibacterial activity, Biomass Conversion and Biorefinery (2023) 1–13.
[16] G.G. Hasan, et al., Efficient treatment of oily wastewater, antibacterial activity, and photodegradation of organic dyes using biosynthesized Ag@ Fe3O4 nanocomposite, Bioproc. Biosyst. Eng. 47 (1) (2024) 75–90.
[17] S. Meneceur, et al., Removal efficiency of heavy metals, oily in water, total suspended solids, and chemical oxygen demand from industrial petroleum wastewater by modern green nanocomposite methods, J. Environ. Chem. Eng. 11 (6) (2023) 111209.
[18] M. Islam, M. Mostafa, Textile dyeing effluents and environment concerns—a review, J Environ Sci Nat Resour 11 (1) (2018) 131–144.
[19] A.S. Rathore, R.D. Gupta, Chitinases from bacteria to human: properties, applications, and future perspectives, Enzym. Res. 2015 (1) (2015) 791907.
[20] K. Tanaka, K. Padermpole, T. Hisanaga, Photocatalytic degradation of commercial azo dyes, Water Res. 34 (1) (2000) 327–333.
[21] S.N.U.S. Bukhari, et al., Psyllium-husk-assisted synthesis of ZnO microstructures with improved photocatalytic properties for the degradation of methylene blue (MB), Nanomaterials 12 (20) (2022) 3568.
[22] M. Azzi, et al., Plant extract-mediated synthesis of Ag/Ag2O nanoparticles using Olea europaea leaf extract: assessing antioxidant, antibacterial, and toxicological properties, Biomass Conversion and Biorefinery (2023) 1–14.

[23] R.S. Sabry, M.I. Rahmah, W.J. Aziz, A systematic study to evaluate effects of stearic acid on superhydrophobicity and photocatalytic properties of Ag-doped ZnO nanostructures, J. Mater. Sci. Mater. Electron. 31 (16) (2020) 13382–13391.

[24] R.S. Sabry, W.J. Aziz, M.I. Rahmah, Employed silver doping to improved photocatalytic properties of ZnO micro/nanostructures, J. Inorg. Organomet. Polym. Mater. 30 (11) (2020) 4533–4543.

[25] M.I. Rahmah, et al., Synthesis of ZnO/Ag-doped C/N heterostructure for photocatalytic application, Int. J. Mod. Phys. B 37 (24) (2023) 2350239.

[26] M.I. Rahmah, H.B. Qasim, A novel method to prepare antibacterial ZnO nanoflowers, Appl. Phys. A 128 (11) (2022) 998.

[27] M. Soosen Samuel, L. Bose, K. George, Optical properties of ZnO nanoparticles, Academic Review 16 (2009) 57–65.

[28] M.A. Bhatti, et al., Efficient photo catalysts based on silver doped ZnO nanorods for the photo degradation of methyl orange, Ceram. Int. 45 (17) (2019) 23289–23297.

[29] G. Murugadoss, Synthesis and characterization of transition metals doped ZnO nanorods, J. Mater. Sci. Technol. 28 (7) (2012) 587–593.

[30] K.-C. Lee, et al., Size effect of Ag nanoparticles on surface plasmon resonance, Surf. Coating. Technol. 202 (22–23) (2008) 5339–5342.

[31] S. Vikal, et al., Structural, optical and antimicrobial properties of pure and Ag-doped ZnO nanostructures, J. Semiconduct. 43 (3) (2022) 032802.

[32] M. Kareem, et al., Synthesis, characterization, and photocatalytic application of silver doped zinc oxide nanoparticles, Cleaner Materials 3 (2022) 100041.

[33] A. El-Bindary, A. Ismail, E. Eladl, Photocatalytic degradation of reactive blue 21 using Ag doped ZnO nanoparticles, J. Mater. Environ. Sci. 10 (12) (2019) 1258–1271.

[34] S.B. Jaffri, K.S. Ahmad, Phytofunctionalized silver nanoparticles: green biomaterial for biomedical and environmental applications, Rev. Inorg. Chem. 38 (3) (2018) 127–149.

[35] H. Xue, et al., Influence of Ag-doping on the optical properties of ZnO films, Appl. Surf. Sci. 255 (5) (2008) 1806–1810.

[36] S. Helen, et al., Temperature-dependent dielectric investigation of dual-ions doped hydroxyapatite nanoparticles, Inorg. Chem. Commun. 158 (2023) 111606.

[37] C.E. Jeyanthi, et al., A comparative study on physico-chemical, optical, magnetic and ferroelectric properties of undoped BiFeO3 and Ni-doped BiFeO3 nanoparticles, Inorg. Chem. Commun. 158 (2023) 111608.

[38] S. Hosseini, et al., Effect of Ag doping on structural, optical, and photocatalytic properties of ZnO nanoparticles, J. Alloys Compd. 640 (2015) 408–415.

[39] F. Khurshid, et al., Ag-doped ZnO nanorods embedded reduced graphene oxide nanocomposite for photo-electrochemical applications, R. Soc. Open Sci. 6 (2) (2019) 181764.

[40] A. Ashwini, et al., Visible light photocatalysis enhancement by Ag3PO4 decorated with RuO2 nanoparticles, Phys. B Condens. Matter 682 (2024) 415890.

[41] S. Kumaresan, K. Vallalperuman, S. Sathishkumar, A Novel one-step synthesis of Ag-doped ZnO nanoparticles for high performance photo-catalytic applications, J. Mater. Sci. Mater. Electron. 28 (2017) 5872–5879.

[42] B.D. Ahn, et al., Synthesis and analysis of Ag-doped ZnO, J. Appl. Phys. 100 (9) (2006).

[43] Ö.A. Yıldırım, H.E. Unalan, C. Durucan, Highly efficient room temperature synthesis of silver-doped zinc oxide (ZnO: Ag) nanoparticles: structural, optical, and photocatalytic properties, J. Am. Ceram. Soc. 96 (3) (2013) 766–773.

[44] T. Chitradevi, A. Jestin Lenus, N. Victor Jaya, Structure, morphology and luminescence properties of sol-gel method synthesized pure and Ag-doped ZnO nanoparticles, Mater. Res. Express 7 (1) (2020) 015011.

[45] H.I. Rizvi, et al., Novel existence of Mn and Cu in WO3 nanostructures for promising photocatalytic activity against MB dye and Levofloxacin antibiotic, J. Alloys Compd. 993 (2024) 174549.

[46] A. Bhosale, et al., Efficient photodegradation of methyl orange and bactericidal activity of Ag doped ZnO nanoparticles, J. Indian Chem. Soc. 100 (2) (2023) 100920.

[47] A. Younas, et al., Novel S–N/WO3: optimization of photocatalytic performance of WO3 by simultaneous existence of S and N in WO3 against MB dye, J. Chem. Phys. 160 (24) (2024).

[48] H.A. Rafaie, et al., Photocatalytic degradation of methylene blue dye solution using different amount of ZnO as a photocatalyst, Science Letters 15 (1) (2021) 1–12.

[49] M.H. Sayed Abhudhahir, J. Kandasamy, Photocatalytic effect of manganese doped WO3 and the effect of dopants on degradation of methylene blue, J. Mater. Sci. Mater. Electron. 26 (11) (2015) 8307–8314.

[50] K.V. Chandekar, et al., Visible light sensitive Cu doped ZnO: facile synthesis, characterization and high photocatalytic response, Mater. Char. 165 (2020) 110387.

[51] R. Akram, et al., Photocatalytic degradation of methyl green dye mediated by pure and Mn-doped zinc oxide nanoparticles under solar light irradiation, Adsorpt. Sci. Technol. 2023 (2023) 5069872.